doi: 10.56761/EFRE2022.S1-O-024202

Ring structure of electron-ion beams ejected by a picosecond high-current electron accelerator

V.I. Baryshnikov[1], V.L. Paperny[2,], A.B. Chernyh[2]*

[1]Irkutsk State Transport University, Irkutsk, Russia
[2]Irkutsk State University, Irkutsk, Russia
[*]paperny@math.isu.runnet.ru

Abstract. The results of a study of the parameters of the radial structure of electron-ion beams emitted by a high-voltage vacuum discharge with an extremely high energy deposition rate > 5×10^{13} A/s are presented. An analysis of the structure of beam imprints on the irradiated anode foil, as well as traces of erosion on the crystalline substrate obtained by the authors earlier, showed that there are rings on a scale of tens of microns, and the energy of accelerated electrons in the central part of the beam is much higher than in the peripheral rings. A possible mechanism providing the observed beam structure is considered.
Keywords: vacuum discharge, accelerated beams, ring structure.

1. Introduction

High-current pulsed vacuum discharges have attracted the attention of researchers for several decades, firstly, due to the variety of physical phenomena observed in them, and secondly, due to numerous applications, for instance, for the generation of high-power UV, VUV and X-ray radiation, accelerated electron beams and multiply charged ions and so on. One of the interesting and little studied phenomena recorded in pulsed vacuum discharges is the ring structure of the beam of electrons and accelerated ions of the cathode material emitted by the discharge towards the anode. In recent years, these beams consisting of a central filament surrounded by concentric annular beams have been found in high-current vacuum spark [1, 2] and accelerators of relativistic electrons with a metal cathode [3]. In these experiments, the diameter of the central filament and the coaxial surrounding rings was a few millimeters [1, 2] or centimeters [3]. The mechanism of the formation of such structures remains a subject of discussion. It seems important to study such a structure of an electron-ion jet emitted by a vacuum discharge cathode, since the peripheral regions of the jet can shunt the main, central current channel and thus significantly affect the plasma pinching process.

Previously, the authors in [4] showed that the imprint on the anode foil of a particle beam emitted by a high-voltage picosecond vacuum discharge with an extreme high energy input rate > 5×10^{13} A/s has the form of concentric rings 2–5 mm in diameter. In this work, further studies of this effect were carried out in order to elucidate the possible mechanism for the formation of such structures.

2. Experimentals

The experiments are performed with a small-size electron accelerator, which is an essentially modified version previously used in [5, 6]. The needle cathode with an apex angle of about 1° is manufactured of a titanium or tungsten rod with a diameter of 1.5 mm. An anode is a Al-film 25 µm thick, which is part of an aluminum coaxial vacuum chamber with a low inductance. The residual pressure in the vacuum chamber is maintained at about 10^{-4} Torr. The increase in pressure to large values of the order of 10^{-3} Torr does not affect the experimental data. The accelerator operating at a pulse repetition rate of 1–6 Hz is constructed on the basis of a hybrid picosecond high voltage generator, which is designed according to the Tesla resonant generator circuit, where the output circuit capacitor is divided into two equal components *C1* and *C2*, which are parts of a two-stage Marx generator. After the switching on of spark gaps *T2* and *T3*, the low-inductance capacitors *C1* and *C2* form the shock capacitor *C*, which loads the vacuum diode through the forming line. An effective power supply of the generator to the vacuum accelerating diode is achieved using special argon-hydrogen high-pressure (40 atm) spark gaps *T2* and *T3*. Capacitors *C1* and *C2* are charged in parallel by the impulse voltage in a time of ~1 μs that increases the electrical strength of the insulating elements of the generator and spark gaps. This allows us to sharply reduce the overall dimensions of the generator (diameter 120 mm, length 350 mm), which led to a decrease in energy losses in both the skin layer, parasitic inductances and capacitances, and in the dynamic resistance of the discharge gaps. Due to this, it is possible to reduce the pulse length and, consequently, to increase the rate of current rise in the pulse. The impedance of the generator is about 30 Ohms.

The photoluminescence spectra are recorded with an ASP-100M 170–1100 nm fiber spectrometer (spectral resolution, 1 nm). To study the kinetics of PL spectra, a spectral complex is used, in the excitation channel of which the second harmonic (440 nm) of a tunable femtosecond TIF-50 laser is used. The luminescence spectrum at the output of the MDR-23 monochromator is recorded using a 31-ELU-detector.

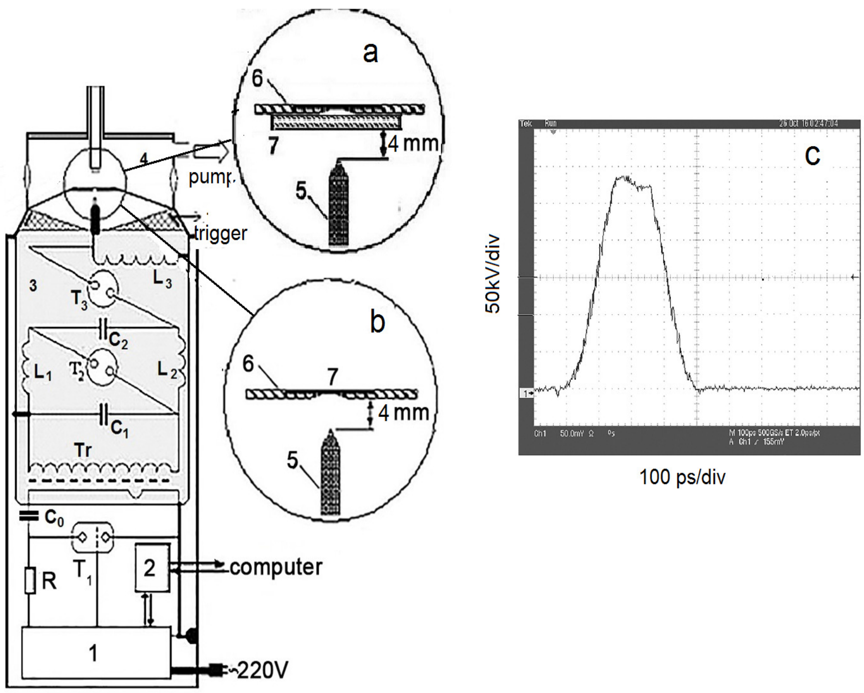

Fig.1. Schematic diagram of the experimental device. (1) High-voltage power supply, (2) microcontroller, (3) picosecond high-voltage generator of the Marx–Tesla type, (4) cryostat with sapphire windows for sample analysis. The inserts show the design of various versions of the accelerating diode: (a) (5) titanium cathode, (6) anode, (7) sapphire substrate; (b) (5) tungsten cathode, (6) anode, (7) titanium foil; (c) waveform of the discharge voltage pulse.

3. Results and discussion

Figure 2a shows a photomicrograph of the surface of a sapphire crystal after irradiation with electron-ion beams in a series of 300 pulses with a repetition frequency of 1 Hz according to the experimental scheme shown in Fig.2a. It can be seen from the figure that luminescence, mainly in the red range of the optical spectrum, is recorded from an annular structure with a diameter of about 30 μm. At the same time, from Fig.2b, where the cross-section along the depth of the irradiated region is depicted, it follows that as a result of irradiation, an erosion crater with a depth of several tens of micrometers is formed on the crystal surface. The edge of the crater radiates in the red range of the spectrum, forming the above-mentioned ring structure, the central area of the crater radiates in the blue range of the spectrum, and in the center of the crater, there is a channel with a diameter of the order of a micrometer, which luminesces in the green range of the spectrum.

To quantitatively analyze the results obtained, the spectrum of this radiation is measured [7]. A broad photoluminescence (PL) band with a maximum at 780 nm, characteristic of Ti^{3+} ions embedded in the lattice sites of Al_2O_3 is recirded. A blue radiation at a wavelength of 450 nm corresponds to the scattered laser radiation. The PL band at 560 nm in the green spectral range is identified as the emission of defects (color centers) in sapphire, which are created by a beam with an electron energy of more than 400 keV

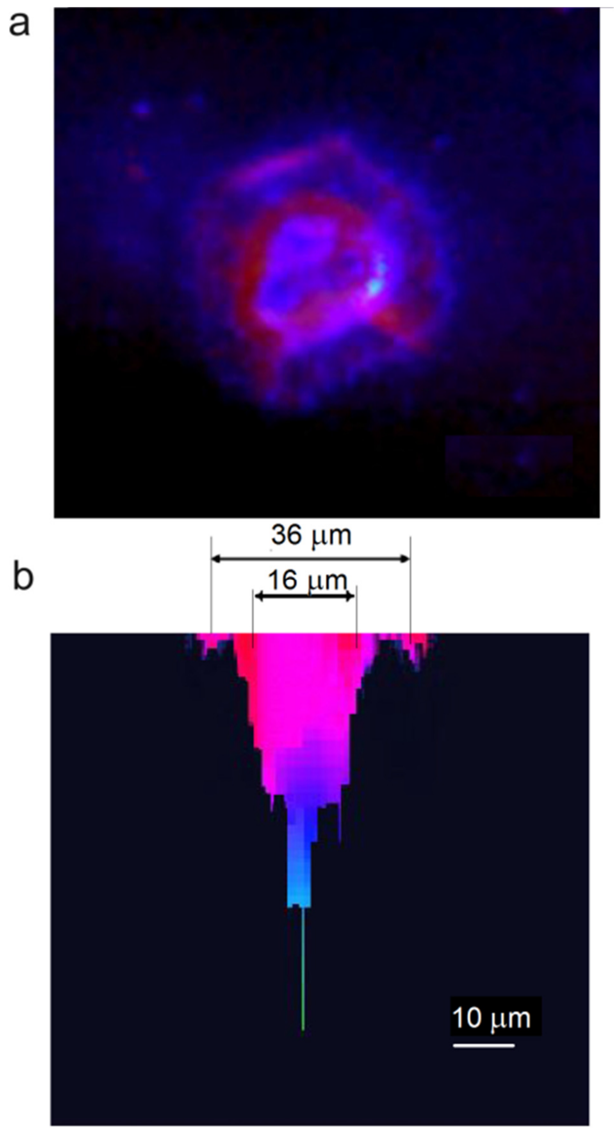

Fig.2. The spatial structure of the luminescent area of a sapphire crystal after treatment with a high-energy electron-ion (Ti^{n+}) beam.

It follows from Fig.2b that the erosion crater has a pronounced discrete structure, namely, it consists of an outer annular crater with a diameter of 36 µm, an inner ring with a diameter of about 16 µm, and a core with a diameter of 4 µm. Hence it follows that the electron-ion beam, which creates the observed structure of the crater, also has the corresponding ring structure.

To obtain additional information about the beam structure, we analyzed the imprint created by the beam on the anode foil, obtained according to the scheme presented in inset (b) of Fig.1. A micrograph of the Al surface of an anode foil of 20 µm thick, irradiated with 5×10^3 pulses of the beam emitted by the W pointed cathode, is shown in Fig.3a. It follows from the figure that the imprint also has a ring structure.

The image was processed as follows: first, the ring areas of the image corresponding to the blue (430–460 nm), green (490–530 nm), yellow (570–600 nm) and red (630–670 nm) spectral ranges were selected by the Photoshop processor. Then, in each spectral range, a sector with an angle of $\pm 30^0$ relative to the horizontal diameter was selected in the image, and the image intensity in this spectral range was averaged over the sector. The obtained radial intensity distributions are depicted by the corresponding colored curves in Fig.3b. Assuming that the resulting photo is an interference pattern formed upon reflection of light from a metal film of variable thickness deposited by a beam on the surface of the anode foil, the radial distribution of the film thickness was estimated.

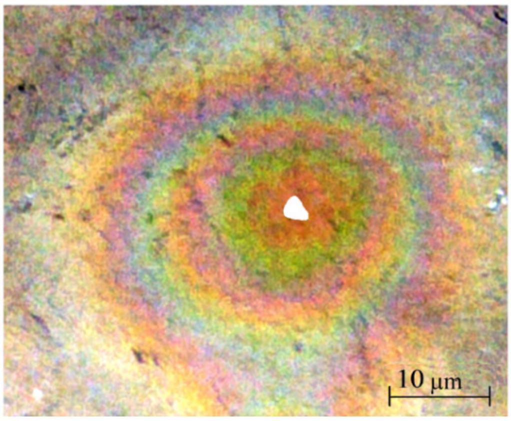

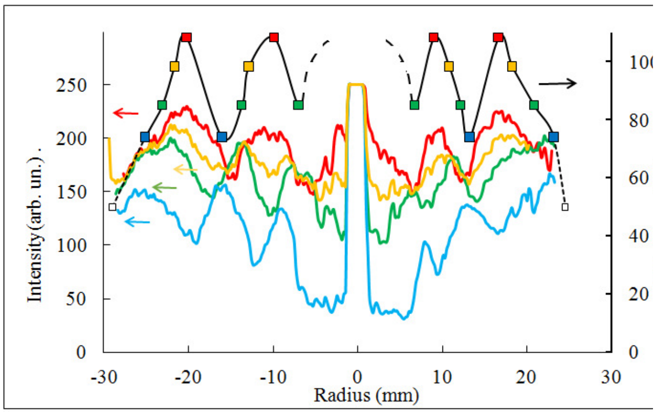

a b

Fig.3. (a) Micrograph of the surface of an anode foil, irradiated with 5×103 pulses of an electron-ion beam emitted by a W needle cathode, The spot in the center is a hole in the foil burned by the electron beam. (b) Radial intensity distributions in micrographs in different spectral ranges, as well as the distribution of the thickness of the W foil deposited on the surface of the anode foil, reconstructed from color plots.

For this, a well-known formula is used that relates the angle with the normal i_1, at which the maximum of the interference pattern is observed, which occurs when a film with a thickness h of a material with a refractive index n is irradiated with light with a wavelength λ_0

$$2h\sqrt{n^2 - sin^2 i_1} = m\lambda_0,$$

Assuming that the observation is carried out along the normal to the substrate surface, i.e. angle $i_1 \approx 0$, for tungsten $n \approx 3$ and the observed pattern corresponds to the first order of interference, i.e. $m = 1$, we calculate the film thickness at radii approximately corresponding to the maxima of the intensity distribution for radiation with an average wavelength in the specified spectral ranges.

The result shown in Fig.3b shows that the observed pattern is a set of two spatially separated rings with maxima at radii of 10 and ~20 µm and a spatially unresolved central maximum. The maximum film thickness is about 100 nm, and this value turned out to be the same for both rings, which indicates a similar density of ions in tubular structures formed in an electron-ion beam. At the same time, since, according to Fig.2a, the depth of the erosion crater of the outer ring is significantly less than the depth of the inner crater, it follows that the energy of the electron beam in the outer ring is less than the energy of the inner tube beam.

This conclusion is also supported by the luminescence spectra of various regions of the crater. Indeed, the luminescence of the outer, with a diameter of 36 μm, and the first inner region of the crater, with a diameter of 16 μm, in the red spectral range means that the radiation source is Ti^{+3} ions embedded by the beam into the nodes of the matrix. Consequently, here the energy of the beam ions exceeds the threshold value of the embedding of titanium ions into the nodes of the sapphire crystal lattice, which is equal to 300 keV. At the same time, the energy of electrons in these regions of the beam turns out to be less than the threshold energy of the formation of intrinsic defects (color centers) in the sapphire matrix, which is 380 keV [8], as a result of which the luminescence of these centers is not observed.

The emission from the central region of the crater in the blue spectral range corresponds to the scattered excitation laser radiation (450 nm), and the emission in the green range of the spectrum corresponds to the emission band with a maximum at $\lambda = 560$ nm of intrinsic defects in the Al_2O_3 matrix created by beam electrons at a sufficiently high energy >400 keV [9]. Consequently, the energy of electrons in the central region of the beam exceeds this threshold value and turns out to be sufficient for the formation of defects that generate radiation in the indicated band. Exciting laser radiation is also scattered on these defects, and, since ions penetrate into the substrate only to a shallow depth <0.5 μm [8], only a thin near-surface layer of the crater radiates in the red region of the spectrum. At the same time, beam electrons with an energy of more than 400 keV create a defect region in the substrate with a depth of about 10 μm, and thus the intensity of the radiation associated with them significantly exceeds the intensity of radiation due to ions.

Comparison of Fig.2 and Fig.3 shows that the structure of the electron-ion beam emitted by the cathode is similar for the cases of Ti and W cathodes, and this structure has the form of concentric tubes and is similar to that observed earlier in works [1–3], but significantly smaller, micron, scale. At present, the mechanism of formation of the tubular structure of the beam is the subject of discussion. The most natural assumption is that the beam ions are spatially separated due to the difference in their Larmor radii as they move in the current's magnetic field of the central, densest region of the beam.

Let us consider the consequences of this assumption. Since for ions of mass m with charge state Z the Larmor radius $r_L \propto m^{1/2}/Z^{1/2}$, then the ring of maximum radius corresponds to ions with $Z = +1$, the radius of the next ring is $2^{0.5} \approx 1.4$ less and etc. In addition, according to this relation, in the case of a tungsten cathode, the radii of the rings are $(m_W/m_{Ti})^{0.5} \approx 1.8$ times larger than the radii of the corresponding rings for a titanium cathode. However, the above experimental results do not correspond to these estimates. Note that in experiments with high-current pinches [1, 2], where the tubular structure of the plasma jet emitted by the cathode was also recorded, the ratio of the radii of the outer tubes was close to two unlike the estimate above.

4. Conclusions

Thus, this work allows us to come to the following conclusions:

1. The electron-ion beam emitted by the cathode of the accelerator with an extremely high energy input rate of > $5 \cdot 10^{13}$ A/s has a structure in the form of set of the concentric tubes (cones) with a diameter of < 40 μm, and the beam densities in the peripheral regions turned out to be close;

2. An analysis of the experimental results, as well as the data of other authors, allows us to conclude that, despite the qualitative agreement between the observed tubular structure of the electron-ion beam and the indicated assumption, evidently, it is also necessary to take into account the magnetic field of currents flowing in external current tubes.

Acknowledgement

This work was supported by the Russian Foundation for Basic Research (grant no. 20-02-00322)

5. References

[1] Dolgov A.N., Klyachin N.A., and Prokhorovich D.E., *Tech. Phys*., **59**, 1881, 2014; doi: 10.1134/S1063784214120044
[2] Lopatin V.S., Remnev G.E., and Martynenko A.A.; *Tech. Phys. Lett.***43,** 463, 2017; doi: 10.1134/s1063785017050212
[3] Kuznetsov A.P., et al., *Plasma Physics Reports*, **34**(3), 193, 2008; doi: 10.1134/S1063780X08030045
[4] Baryshnikov V.I., Paperny V.L., and Shipayev I.V., *J. Phys. D: Appl. Phys.*, **50,** 425206, 2017; doi: 10.1088/1361-6463/aa85c4
[5] Baryshnikov V.I., Paperny V.L., *Russ. Phys. Tech. Phys. Lett.*, **21**, 40, 1995;
[6] Baryshnikov V.I., Paperny V.L., *J. Phys. D: Appl. Phys.*, **28**, 2519, 1995; doi: 10.1088/0022-3727/28/12/019
[7] Baryshnikov V.I., and Paperny V.L., *Physics of Plasmas*, **25**, 083106 2018; doi: 10.1063/1.5033364
[8] Komarov F.F., *Phys. Usp.*, **46**, 1253, 2003; doi: 10.1070/PU2003v046n12ABEH001286
[9] Pells G.P., and Phillips D.C., *J. Nucl. Mater.,* **80**, 207, 1979; doi: 10.1016/0022-3115(79)90183-1